# Full 3D Coverage Beamforming Phased Array with Reduced Phase Shifters and Control 2D Tunable 3 × 3 Nolen Matrix

Hanxiang Zhang
Department of Electrical and Computer Engineering
Florida A&M University - Florida State University
Tallahassee, Florida, USA
hz21c@fsu.edu

Bayaner Arigong
Department of Electrical and Computer Engineering
Florida A&M University - Florida State University
Tallahassee, Florida, USA
barigong@eng.famu.fsu.edu

Abstract—In this paper, a 3D beamforming phased array with 2D stacked tunable Nolen matrix is presented. The fundamental building block - tunable Nolen matrix is proposed to relax phase tuning range of phased shifters and reduce the complexity of control mechanism by embedding tunable phase shifters within Nolen matrix. For each input port excitation of proposed tunable Nolen network, a tunable progressive phase difference within range of  $120^{\circ}$  is obtained at its output ports, and full  $360^{\circ}$  range is achieved by exciting all three input ports. By stacking and cascading six  $3 \times 3$  Nolen matrices, nine radiation beams in unique cubic sector can be continuously steered on azimuth and elevation planes, realizing full 3D beamforming function. To verify the design concept, the network has been simulated at 5.8GHz, and the simulation results agree well with theoretical analysis.

Keywords— Feeding network, 3D tunable beamforming, phase relaxed, microwave circuits, phased array.

### I. INTRODUCTION

Time, frequency spectrum, coding, and space are available resource for high performance wireless communication, and the demand for high data rate and increasing system capacity push spatial domain resource more important than ever, especially with emerging 5G/NextG, low earth orbit (LEO), autonomous driving radar etc. Spatial multiplexing and beam-space multiplexing approaches have been intensively investigated to increase system capacity, signal to noise ratio, power gain, frequency reuse in given area, and interference suppression by utilizing beamforming techniques which combine multiple antennas in a smart array form to reshape the waveform by controlling magnitude and phase and radiate it into desired direction as well to suppress the gain into angular of interference signals.

To implement beamforming in hardware domain, digital beamforming [1]-[3], LO phase shifting [4]-[5], and RF phase shifting [6]-[7] are primary techniques to form and continuously steer the radiation beams as desired will. In RF phase shifting, feeding antenna elements with progressive phase difference plays major role to control beamforming angle, where several methods have been investigated, such as series feeding [8]-[10], parallel feeding [11]-[12], and matrix feeding [15]-[16]. Compared with series and parallel feeding, the matrix feeding network is composed of components like couplers, phase shifters [17], crossovers, and power combiners. Butler matrix is

one of the well-known feeding networks featuring symmetrical & unsymmetrical topology and has been designed in different scales as well [18]-[22]. To break the fixed radiation angle of conventional butler matrix, our previous work [23]-[24] proposed a tunable  $4 \times 4$  Butler matrix to tune the progressive phase delay continuously using two embedded phase shifters with phase tuning range in  $90^{\circ}$  and  $180^{\circ}$ .

With increasing number of antenna elements in beamforming array, it needs a smaller number of passive components as coupler, crossover, delay line, and phase shifter in feeding network to minimize power loss in energy limited RF front end, especially for mm-Wave and THz communications. Comparing with other feeding network as Butler and Blass matrix, Nolen matrix shows more advantages, i.e., fewer components, low loss, compact size, and more flexible to generate arbitrary number of radiation beams, which caters for large scale beamforming array. In our previous work [25]-[28], Nolen matrix has been investigated to generate flexible beams and reduce the size. However, all our work has focused on fixed radiation beams without any tuning capabilities. Also, with strong needs for full spatial domain utilization in NextG, 3D beamforming attracts more interest than linear 2D beamforming array to boost capability of identifying users in full spatial domain by generating beam in cubic coverage area.

In this paper, a novel 2D tunable Nolen matrix as in Fig. 1 is proposed to generate and steer beam in full 3D spatial domain for next generation spatial and beam-space multiplexing wireless applications. The features of proposed 3D beamforming array are: 1) flexible progressive phase difference in horizontal and vertical antenna array; 2) using tunable phase shifter with only 120° tuning range to realize full 360° progressive phase difference in two planes; 3) all the phase shifters are designed to embed into feeding network; 4) applying only two-channel voltages to concurrently control all beamforming; 5) 3D cubic space coverage enables further extension of system channel capacity. This paper is organized as follows. In section II, closed-form equations are derived for proposed tunable 3 × 3 Nolen matrix. In section III, the simulation and experiment are carried to validate proposed design, and contour diagrams of full 3D beamforming is simulated to demonstrate our proposed design concept. Finally, in section IV, the conclusion and future works are briefly discussed.

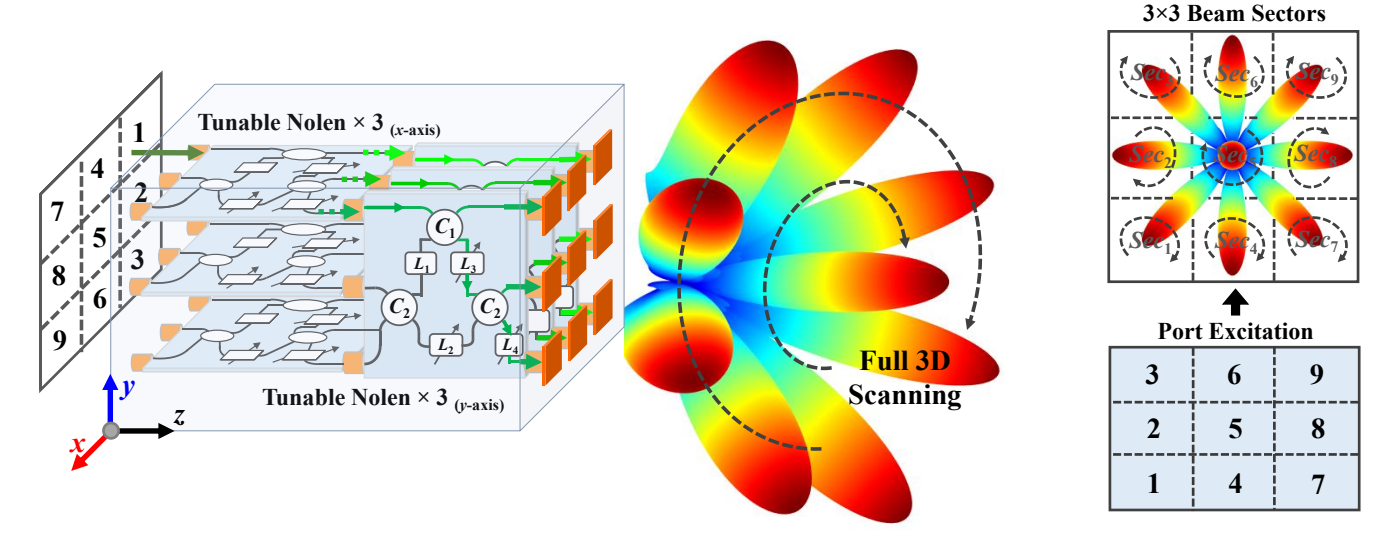


Fig. 1 Schematic of the proposed 3D beamforming phased array composed of stacked 2D tunable  $3 \times 3$  Nolen matrices. Each beam is excited by corresponding input port  $1 \sim 9$  and steered within full progressive phase difference range  $360^{\circ}$ .

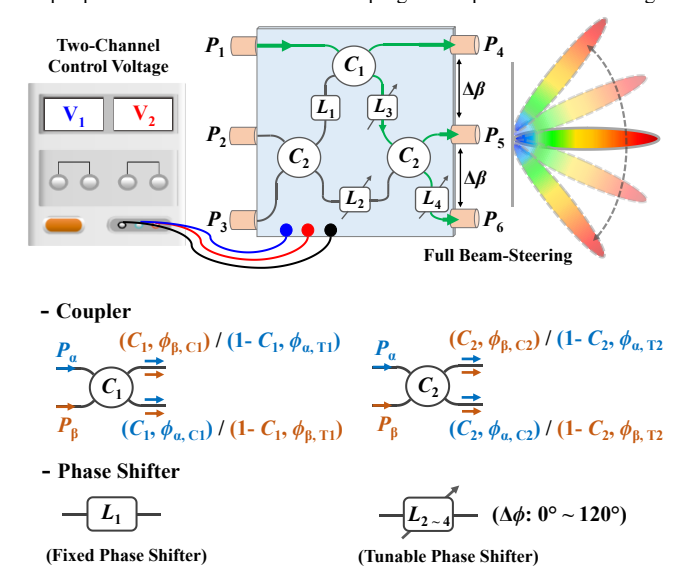


Fig. 2 Schematic diagram of single  $3 \times 3$  fully tunable Nolen matrix with two-channel control voltages to realize full beamforming.

### II. THEORETICAL ANALYSIS

The proposed full coverage 3D beamforming phased array using novel tunable  $3 \times 3$  Nolen matrix is shown in Fig. 1. Three matrices are stacked on y - axis, and another three are piled up along x - axis. Applying signal at one port, the equal magnitude and progressive phase delay  $(\beta_x, \beta_y)$  in two dimensions are generated. The signals from output of two-dimensional matrices are fed into the nine-element antenna array to generate radiation beam at a direction in cubical 3D space. Nine unique radiation beams located in corresponding cubic sectors can be generated by switching different input ports. Furthermore, to fully cover 3D space in each sector or to radiate beam in any angle direction within cubic sector, the two-channel voltages tune the phases shifters in Nolen matrix to generate progressive phase difference  $(\beta_x, \beta_y)$  with 360° range at its output ports,

where all the phase shifters are controlled simultaneously to relax control mechanism.

### A. Tunable 3 × 3 Nolen Matrix

The fundamental building block - tunable 3 × 3 Nolen matrix is a microwave network with three input ports  $(P_1 - P_3)$  and three output ports  $(P_4 - P_6)$ , as shown in Fig. 2. It is composed three couplers with two different coupling ratios  $C_1$  and  $C_2$ , three tunable phase shifters  $(L_2, L_3, \text{ and } L_4)$  with phase tuning range of  $\phi_2, \phi_3, \phi_4$ , and one fixed phase shifter  $L_1$  (phase delay =  $\phi_1$ ). More specifically, when port  $P_{\alpha}$  of coupler 1 is excited, the signal at coupling port is  $C_1$ , and phase delay is  $\phi_{\alpha,C_1}$ . While the signal at through port has magnitude of  $(1 - C_1)$  and phase delay  $\phi_{\alpha,T_1}$ . Similarity, when  $P_{\beta}$  is excited, the same magnitude distributions can be achieved, and the phase delays are  $\phi_{\beta,C1}$  and  $\phi_{\beta,T1}$ , respectively. For other two couplers having coupling ratio of  $C_2$ , the corresponding magnitudes and phase delays under different port excitations are shown in Fig. 2 as well. More details about coupler design have been discussed in our previous research work [27]. In this design, the phase differences of couplers under different port excitations can be expressed as:

$$(\phi_{\alpha,C1} - \phi_{\alpha,T1}) + (\phi_{\beta,C1} - \phi_{\beta,T1}) = \pi \tag{1}$$

$$(\phi_{\alpha,C2} - \phi_{\alpha,T2}) + (\phi_{\beta,C2} - \phi_{\beta,T2}) = \pi$$
 (2)

Also, the corresponding coupling ration  $C_1$  and  $C_2$  are derived respectively to 2/3 and 1/3 by considering the requirement of equal magnitude distribution and progressive phase differences across the entire matrix [25]. Therefore, the *S*-parameters of the  $3 \times 3$  network is derived as:

$$S_{41} = \frac{\sqrt{3}}{3} e^{j\phi_{\alpha,T1}} \tag{3}$$

$$S_{51} = \frac{\sqrt{3}}{3} e^{j(\phi_{\alpha, T2} + \phi_{\alpha, C1} - \phi_3)} \tag{4}$$

$$S_{61} = \frac{\sqrt{3}}{3} e^{j(\phi_{\alpha,C1} + \phi_{\alpha,C2} - \phi_3 - \phi_4)}$$
 (5)

$$S_{42} = \frac{\sqrt{3}}{3} e^{j(\phi_{\alpha,T_1} + \phi_{\beta,C_1} - \phi_1)}$$
 (6)

$$S_{52} = \frac{\sqrt{12}}{12} e^{j(\phi_{\beta,T_1} + 2\phi_{\alpha,T_2} - \phi_1 - \phi_3)} + \frac{1}{2} e^{j(\phi_{\alpha,C_2} + \phi_{\beta,C_2} - \phi_2)}$$
(7)

$$S_{62} = \frac{\sqrt{12}}{12} e^{j(\phi_{\beta,T1} + \phi_{\alpha,T2} + \phi_{\alpha,C2} - \phi_1 - \phi_3 - \phi_4)} + \frac{1}{2} e^{j(\phi_{\beta,T2} + \phi_{\alpha,C2} - \phi_2 - \phi_4)}$$
(8)

$$S_{43} = \frac{\sqrt{3}}{3} e^{j(\phi_{\beta,C1} + \phi_{\beta,C2} - \phi_1)}$$
 (9)

$$S_{53} = \frac{\sqrt{12}}{12} e^{j(\phi_{\beta,T1} + \phi_{\alpha,T2} + \phi_{\beta,C2} - \phi_1 - \phi_3)} + \frac{1}{2} e^{j(\phi_{\beta,T2} + \phi_{\beta,C2} - \phi_2)}$$
(10)

$$S_{63} = \frac{\sqrt{12}}{12} e^{j(\phi_{\beta,T1} + \phi_{\beta,C2} + \phi_{\alpha,C2} - \phi_1 - \phi_3 - \phi_4)} + \frac{1}{2} e^{j(2\phi_{\beta,T2} - \phi_2 - \phi_4)}$$
(11)

For excitation of each input port, the following conditions as equal magnitudes, progressive phase distributions, and unique phase differences are required to steer the radiation beam in its dedicated sector. To satisfy required conditions, the fixed and tunable phase shifters are derived as:

$$\phi_2 - \phi_4 - \phi_1 = \phi_{\beta C2} - \phi_{\beta C1} \mp 90^{\circ}$$
 (12)

$$\phi_3 - \phi_4 = (\phi_{\alpha,C1} - \phi_{\alpha,T1}) - (\phi_{\alpha,C2} - \phi_{\alpha,T2}) + \phi_{\alpha,T2}$$
 (13)

Then, by substituting equations (12) - (13) into (3) - (11), the progressive phase differences of proposed tunable  $3 \times 3$  Nolen matrix are obtained as:

$$\Delta \beta_1 = (\phi_{\alpha C2} - \phi_{\alpha T2}) - \phi_4 \tag{14}$$

$$\Delta \beta_2 = (\phi_{\alpha C2} - \phi_{\alpha T2}) \pm 120^{\circ} - \phi_4 \tag{15}$$

$$\Delta \beta_3 = (\phi_{\alpha C2} - \phi_{\alpha T2}) \mp 120^{\circ} - \phi_4 \tag{16}$$

Where  $\Delta \beta_i$  denotes the progressive phase differences among the output ports when applying incident wave on port 1 to port 3 of  $3 \times 3$  Nolen matrix, respectively. It is observed that  $\Delta \beta_i$  are determined by  $\phi_{\alpha,C2}$  -  $\phi_{\alpha,T2}$  (phase difference of coupler 2) and phase delay  $\phi_4$ . For given coupler, the  $\phi_{\alpha,C2}$  -  $\phi_{\alpha,T2}$  is a predetermined constant value. With this fact, it is easy to find that tuning the phase ( $\phi_4$ ) of phase shifter  $L_4$  will enable continuous progressive phase difference change in proposed matrix. From (14) - (16),  $\Delta \beta_i$  feature 120° offset from each other under each input port excitation (i.e.  $\Delta\beta_2 - \Delta\beta_1 = \Delta\beta_3 - \Delta\beta_2 = \Delta\beta_1 - \Delta\beta_3 = \pm$ 120°), which further reduces required tuning range of tunable phase shifter L<sub>4</sub> from 360° to 120° without decreasing full coverage range of 360°. In addition,  $\phi_2$  and  $\phi_3$  tunable phase shifters must follow the change of  $\phi_4$  with same value or fixed offset, which reduce complexity of control method in proposed beamforming phased array.

From the above analysis, the couplers in the proposed  $3 \times 3$  tunable Nolen matrix are designed from our previous work [29]. After determining the couplers, the phase differences of each coupler ( $\phi_{\alpha,C1}$  -  $\phi_{\alpha,T1}$  &  $\phi_{\alpha,C2}$  -  $\phi_{\alpha,T2}$ ) can be obtained, and phase shifters  $L_1$ ,  $L_2$ ,  $L_3$ , and  $L_4$  can be derived by applying (12) - (13).

To achieve continuous phase tuning with simplified control, a tunable transmission line in our previous design [30] has been

applied to design tunable phase shifters. It consists of two identical microstrip lines in series and three short-end varactors at two ends and center. Here, MA46H120 varactor is adopted as tunable capacitor, and phase tuning is controlled by two bias voltages. Two proposed phase shifters are cascaded to implement tunable phase shifters ( $L_2$ ,  $L_3$  and  $L_4$  in Fig. 2), where its phase tuning range is 120° within low loss variation.

# B. 2-D Phased Array for Full Beamforming

To realize the full coverage 3D beamforming, six of proposed  $3 \times 3$  tunable Nolen matrices are stacked and cascaded to form a 2D antenna feeding network. From Fig. 1, three tunable Nolen matrices are installed on x - axis, while other three are on y - axis. Therefore, there are nine input and nine output ports in this feeding network, and the output ports are connected to a 2D patch antenna array. The array factor (AF) of a planar  $M \times N$  antenna array that excited by incident waves with identical magnitude is derived as

$$AF_{M\times N} = \sum_{m=1}^{M} e^{j(m-1)(k\cdot dx \cdot \sin\theta \cos\phi + \beta_x)} \cdot \sum_{n=1}^{N} e^{j(n-1)(k\cdot dy \cdot \sin\theta \sin\phi + \beta_y)}$$
(17)

where k is wavenumber, dx and dy are distance between the adjacent antenna elements along x - and y - axes,  $\beta_x$  and  $\beta_y$  are progressive phase differences between adjacent antenna elements on x - and y - axes, and  $\theta$  and  $\phi$  are the radiation beam angles on elevation and azimuth dimensions, respectively. The radiation angle of main beam on two dimensions can be derived from the equations:

$$k \cdot dx \cdot \sin \theta \cdot \cos \phi + \beta_{x} = 0 \tag{18}$$

$$k \cdot dy \cdot \sin \theta \cdot \sin \phi + \beta_{y} = 0 \tag{19}$$

With excitation of nine different input ports 1-9, the progressive phase differences of proposed 2D tunable Nolen matrix feeding network on x - and y - axes ( $\beta_x$  and  $\beta_y$ ) are listed in Table I. In specific, there is 120° phase separation between each set of  $\beta_{x,y}$  by exciting the input port in sequence, and  $\beta_x$  and  $\beta_y$  both have independent tuning range of 120°. Based on (18) and (19), the main beams pointing toward nine unique directions in 3D space, and each beam in cubic sector can further be steered by controlling tunable phase.

TABLE I. PROGRESSIVE PHASE DIFFERENCE AND SELECTION OF RADIATION SECTOR UNDER APPLIED INPUT PORTS

Port Excitation	Progressive Phase $(\beta_x, \beta_y)$	Radiation Sector Select
1	(-90°, -90°)	$Sec_1$
2	(-90°, 30°)	Sec <sub>2</sub>
3	(-90°, 150°)	Sec <sub>3</sub>
4	(30°, -90°)	Sec <sub>4</sub>
5	(30°, 30°)	Sec <sub>5</sub>
6	(30°, 150°)	Sec <sub>6</sub>
7	(150°, -90°)	Sec <sub>7</sub>
8	(150°, 30°)	Sec <sub>8</sub>
9	(150°, 150°)	Sec <sub>9</sub>

### III. EXPERIMENTAL RESULTS

To verify theory of our proposed 2D tunable Nolen matrix and 3D beamforming, the simulation has been conducted using Keysight ADS. A 5.8 GHz tunable 3  $\times$  3 Nolen matrix is designed and fabricated on Rogers RT/Duroid 6002 laminate, which has thinks of 0.508mm,  $\tan\delta$  of 0.0012, and dielectric constant  $\varepsilon_r = 2.94$ , as shown in Fig. 5 (a).

# A. S-parameter of 3×3 Tunable Nolen Matrix

In simulation results, all output ports experience an ideal insertion loss of 9.54dB at center frequency 5.8 GHz. As shown in Fig. 3, the progressive phase differences are plotted in both x and y dimensions ( $\beta_x$  and  $\beta_y$ ) for excitations of nine input ports, where solid and dash lines denote limits of phase tuning range ( $\Delta\beta = 120^{\circ}$  contributed from the tunable phase shifters), blue and red curves indicate progressive phase differences along x and y axes. In Fig. 3 (a), for excitation on input port  $P_1$ , the progressive phase differences between two adjacent outputs are tuned between -90° and -210° in both dimensions. In Fig. 3 (b), for input port  $P_2$ ,  $\beta_x$  is tuned from -210° to -90° while  $\beta_y$  is tuned from -90° to 30°. In Fig. 3 (c), for input port  $P_3$ ,  $\beta_x$  keep the same tuning range while  $\beta_y$  is tuned from 30° to 150°. It is observed

that the excitations on ports along vertical axis result into an increase of  $\beta_y$  (from -210° to 150°), which covers the full range of progressive phase differences. On the other hand, for the ports along horizontal axis (i.e.,  $P_1$ ,  $P_4$  and  $P_7$ ),  $\beta_x$  is tuned from -210° to 150° with no change on  $\beta_y$ . Therefore, by exciting the nine input ports ( $P_1$  to  $P_9$ ) and tuning the phase shifters, the beam can be radiated in full 3D space.

# B. 3D Beamforming

Based on above analysis, our proposed 2D tunable Nolen matrix enables generating radiation beam in 3D space. In specific, by sequentially exciting nine input ports, the corresponding radiation sectors can be selected, and the radiation beams in that sector can be continuously steered within the cubic region by tuning the phase shifters. As shown in Fig. 4, the radiation beam having normalized gain within each sector is plotted on azimuth (Az) and elevation (El) dimensions. The specified coordinates are simulated based on the equations (18) and (19). For example, when the input port  $P_5$  is excited, the radiation beam is generated within the region of center sector, and it can be radiated to any angle in that cubic region. Here, in Fig. 4, four beams in clockwise direction as  $(28^{\circ}, 45^{\circ})$ ,  $(28^{\circ}, 45^{\circ})$ 

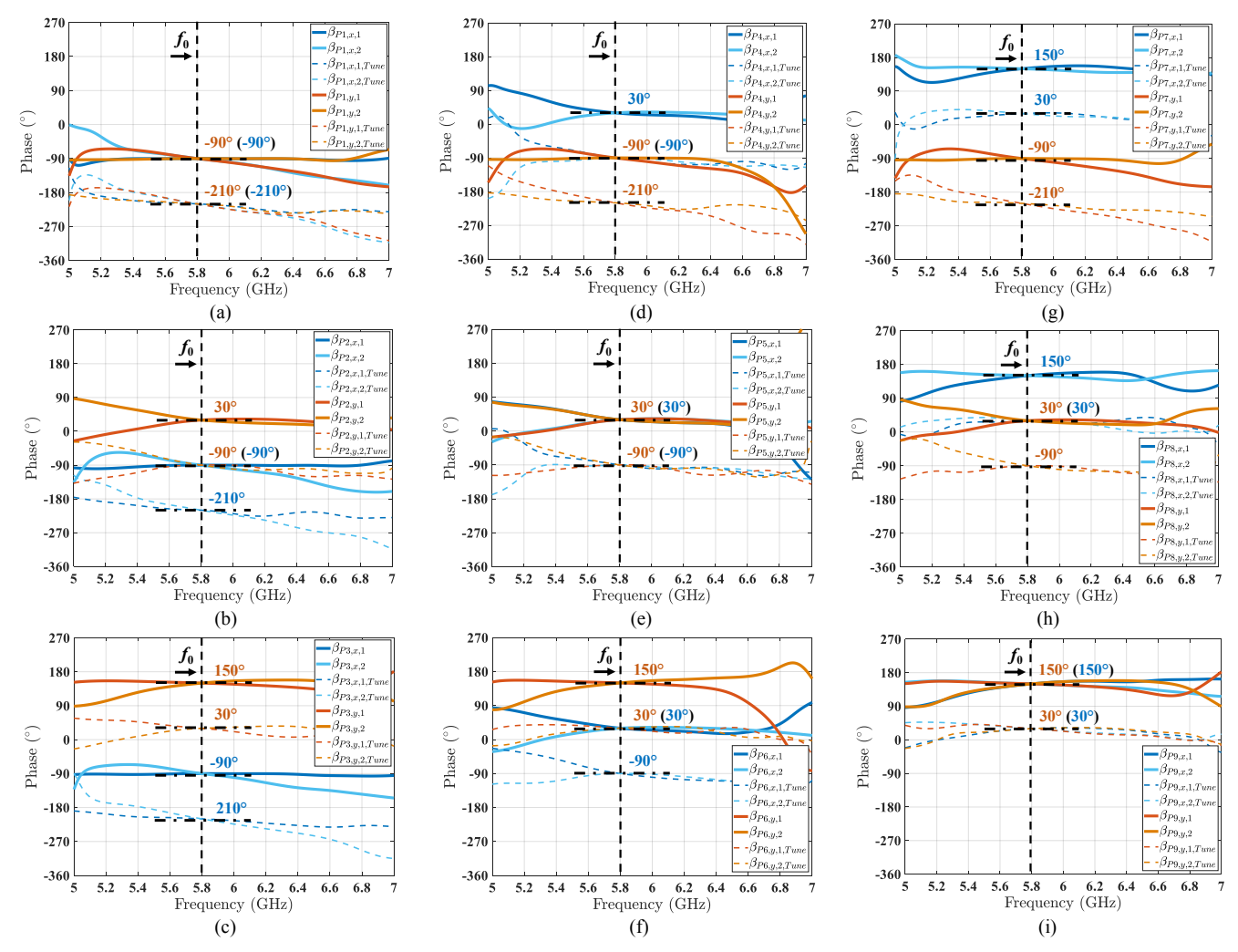


Fig. 3 Simulation results of the proposed 2-D tunable Nolen matrix with excitation from port 1 to port 9: (a) port 1 excitation; (b) port 2 excitation; (c) port 3 excitation; (d) port 4 excitation; (e) port 5 excitation; (f) port 6 excitation; (g) port 7 excitation; (h) port 8 excitation; (i) port 9 excitation.

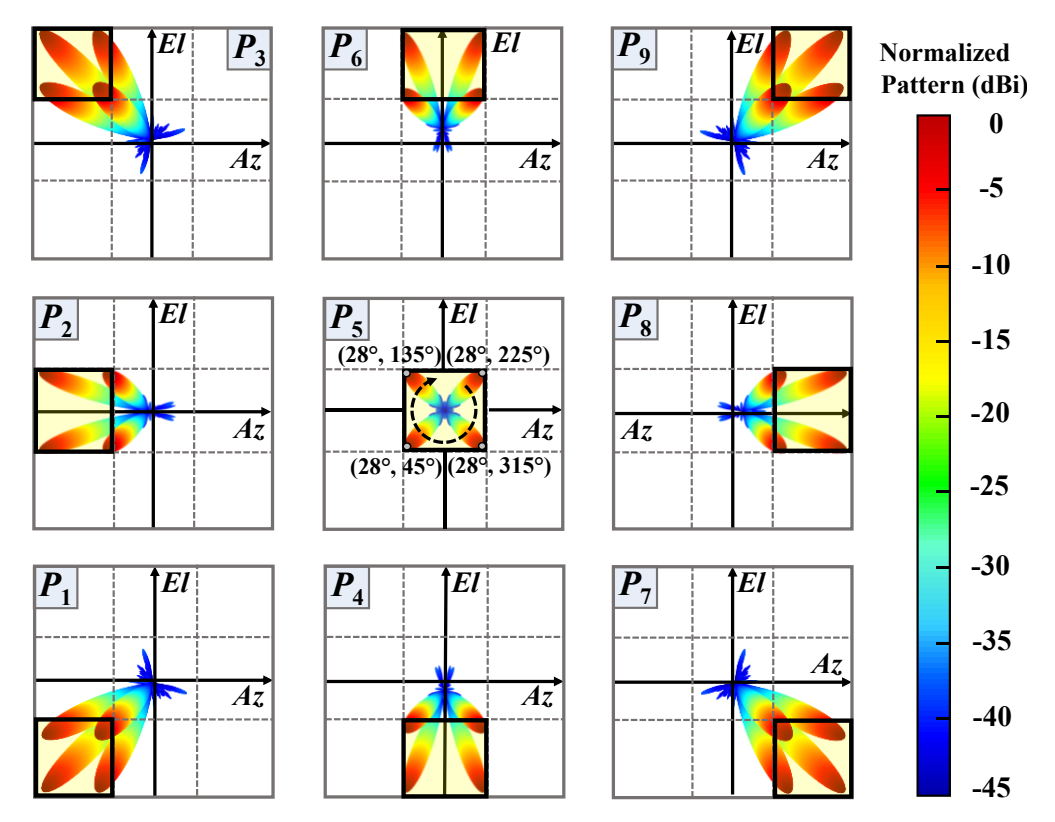
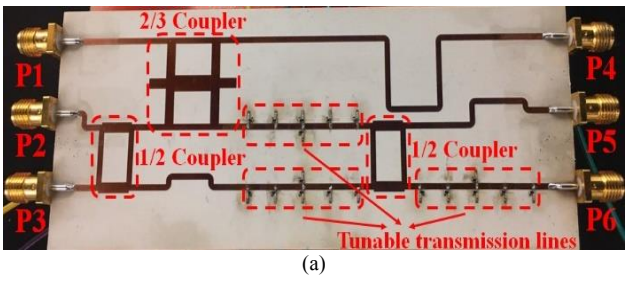


Fig. 4 Antenna beams in nine unique radiation sectors by exciting nine input ports: P<sub>1</sub> to P<sub>9</sub>, continuous steering is achieved from tunable phase shifters.



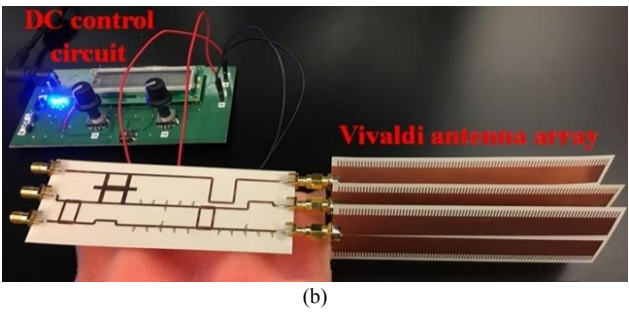


Fig. 5. (a) Photograph of the fabricated 3×3 tunable matrix feeding network, (b) photograph of proposed tunable matrix fully tunable beamforming array.

135°), (28°, 225°), and (28°, 315°) are shown to demonstrate our design concept. Similarly, any radiation beam angle within their dedicated sectors can be generated by tuning phase shifters embedded in proposed design.

# C. Fabrication of 3 × 3 Tunable Nolen Matrix

To verify our design concept, a tunable  $3\times3$  Nolen matrix operating at  $5.8 \, \text{GHz}$  is designed and fabricated on Rogers RT/Duroid 6002 laminate, which has 0.508 mm thickness, 0.0012 loss tangent, and 2.94 dielectric constant shown in Fig. 5(a)). The overall size of the tunable Nolen matrix is about  $113.59 \, \text{mm} \times 34.25 \, \text{mm}$ , which equals to  $2.19 \, \lambda \times 0.66 \, \lambda \, (\lambda \, \text{is}$  the wavelength of  $5.8 \, \text{GHz}$ ). The fabricated tunable  $3 \times 3$  beamforming phased array is shown in Fig. 5(b), where it includes tunable Nolen matrix, Vivaldi antenna array, and control circuit. The control circuit was designed in our previous work [30]. In extended journal paper, more details about measured results of proposed 3D beamforming array will be discussed.

# IV. CONCLUSION

In this paper, a novel 3D beamforming network based on 2D tunable  $3\times3$  Nolen matrix with relaxed phase tuning and simple control is proposed. It realizes equal magnitude and continuous phase differences between adjacent outputs by exciting different input ports. Based on theoretical analysis, it is found that the proposed beamforming network requires tunable phase shifters with small phase tuning range (120°) and only two control voltages to steer the beam covering whole scanning angle in 3D space domain. Our design method can be widely applied in next generation spatial multiplexing and beam-space multiplexing wireless communication with power limited RF front end. In extended work, we will demonstrate proposed 3D beamforming in experiment and correlate with design theory.

### REFERENCES

- [1] D. S. Goshi, Y. Wang, and T. Itoh, "A compact digital beamforming SMILE array for mobile communications," *IEEE Trans. Microw. Theory Tech.*, vol. 52, no. 12, pp. 2732–2738, Dec. 2004
- [2] J. Zhang, W. Wu, and Da. -G. Fang, "Single RF channel digital beamforming multibeam antenna array based on time sequence phase weighting," *IEEE Antennas Wireless Propag. Lett.*, vol. 10, pp. 514–516, May 2011.
- [3] B. Yang, Z. Yu, J. Lan, R. Zhang, J. Zhou, and W. Hong, "Digital beamforming-based massive MIMO transceiver for 5G millimeterwave communications," *IEEE Trans. Microw. Theory Tech.*, vol. 66, no. 7, pp. 3403–3418, July. 2018.
- [4] Y. Soliman and R. Mason, "Application of subharmonic injection locking of LC oscillators to LO-based phase-shifting phased-array architectures," *IEEE Trans. Microw. Theory Techn.*, vol. 58, no. 12, pp. 3475–3484, Dec. 2010
- [5] S. Farzaneh, and A. R. Sebak, "A novel amplitude-phase weighting for analog microwave beamforming," *IEEE Trans. Antennas Propag.*, vol. 54, no. 7, pp. 1997–2008, Jul. 2006.
- [6] T. -W. Li, and H. Wang, "A millimeter-wave fully integrated passive reflection-type phase shifter with transformer-based multi-resonance loads for 360° phase shifting," *IEEE Trans. Circuits Syst. I*, vol. 65, no. 4, pp. 1406-1419, Nov. 2017.
- [7] R. M. Catoira, J. Brégains, J. A. G. Naya, and L. Castedo, "Analog beamforming using time-modulated arrays with digitally preprocessed rectangular sequences," *IEEE Antennas Wireless Propag. Lett.*, vol. 17, no. 3, pp. 497–500, Mar. 2018.
- [8] D. C. Jenn, and S. Lee, "Inband scattering from arrays with series feed networks," *IEEE Trans. Antennas Propag.*, vol. 43, no. 8, pp. 867–873, Aug. 1995.
- [9] H. Mirzaei, and G. V. Eleftheriades, "Arbitrary-angle squint-free beamforming in series-fed antenna arrays using non-foster elements synthesized by negative-group-delay," *IEEE Trans. Antennas Propag.*, vol. 63, no. 5, pp. 1997–2010, May 2015.
- [10] D. Ren, J. H. Choi, and T. Itoh, "Series feed networks for dualpolarized frequency scanning phased array antenna based on composite right/lefthanded transmission line," *IEEE Trans. Microw. Theory Tech.*, vol. 65, no. 12, pp. 5133–5143, Dec. 2017.
- [11] D. C. Jenn, and V. Flokas, "In-band scattering from arrays with parallel feed networks," *IEEE Trans. Antennas Propag.*, vol. 44, no. 2, pp. 172– 178, Feb. 1996.
- [12] A. U. Zaman, and P. –S. Kildal, "Wide-band slot antenna arrays with single-layer corporate-feed network in ridge gap waveguide technology," *IEEE Trans. Antennas Propag.*, vol. 62, no. 6, pp. 2992–3001, Jun. 2014.
- [13] T. Macnamara, "Simplified design procedures for Butler matrices incorporating 90° hybrids or 180° hybrids," *IEEE Proc. H., Microw., Antennas Propag.*, vol. 134, no. 1, pp. 50–54, Feb. 1987.
- [14] P. Chen, W. Hong, Z. Kuai, and J. Xu, "A double layer substrate integrated waveguide Blass matrix for beamforming applications," *IEEE Microw. Wireless Compon. Lett.*, vol. 19, no. 6, pp. 374–376, Jun. 2009.
- [15] N. J. G. Fonseca, "Printed S-band 4 × 4 Nolen matrix for multiple beam antenna applications," *IEEE Trans. Antennas Propag.*, vol. 57, no. 6, pp. 1673–1678, Jun. 2009.

- [16] H. Zhang, B. Arigong, "A Uni-Planar Feeding Network for Monopulse Tracking Radar," 2018 IEEE International Symposium on Antennas and Propagation & USNC/URSI National Radio Science Meeting, Boston, MA, USA, pp.957-958, 2018.
- [17] H. Zhang, H. Ren, H. Tang, B. Zheng, B. Katz, B. Arigong, H. Zhang, "A Microstrip Line Reflection-Type Phase Shifter for 60GHz Phased Array," 2019 IEEE/MTT-S International Microwave Symposium (IMS), Boston, MA, USA, pp. 826 –829, 2019.
- [18] C.-H. Tseng, C.-J. Chen, and T.-H. Chu, "A low-cost 60-GHz switchedbeam patch antenna array with Butler matrix network," *IEEE Antennas Wireless Propag. Lett.*, vol. 7, pp. 432–435, 2008.
- [19] B. Cetinoneri, Y. A. Atesal, and G. M. Rebeiz, "An 8 × 8 Butler matrix in 0.13-µm CMOS for 5–6-GHz multibeam applications," *IEEE Trans. Microw. Theory Techn.*, vol. 59, no. 2, pp. 295–301, Feb. 2011.
- [20] R. D. Cerna and M. A. Yarleque, "A 3D compact wideband 16 × 16 Butler matrix for 4G/3G applications," in *IEEE MTT-S Int. Microw. Symp. Dig.*, Dec. 2018, pp. 16–19.
- [21] M. Koubeissi, C. Decroze, T. Monediere, and B. Jecko, "Switched-beam antenna based on novel design of Butler matrices with broadside beam," *Electron. Lett.*, vol. 41, no. 20, pp. 1097–1098, Sep. 2005.
- [22] Q. Shao, F. C. Chen, Q. X. Chu, and M. J. Lancaster, "Novel filtering 180° hybrid coupler and its application to 2×4 filtering Butler matrix," *IEEE Trans. Microw. Theory Techn.*, vol. 66, no. 7, pp. 3288–3296, Jul. 2018.
- [23] H. Ren, P. Li, Y. Gu, and B. Arigong, "Phase shifter -relaxed and control -relaxed continuous steering multiple beamforming 4×4 Butler matrix phased array," *IEEE Trans. Circuits Syst. I*, Reg. Papers, vol. 67, no. 12, pp. 5031 -5039, Jul. 2020.
- [24] H. Ren, P. Li, Y. Gu, and B. Arigong, "Phase shifter -relaxed and control -relaxed continuous tuning 4×4 Butler matrix," 2020 IEEE/MTT-S International Microwave Symposium (IMS), Los Angeles, CA, USA, pp. 976–979, 2020.
- [25] H. Ren, H. Zhang, Y. Jin, Y. Gu, and B. Arigong, "A novel 2 -D 3×3 Nolen matrix for 2 -D beamforming applications," *IEEE Trans. Microw. Theory Techn.*, vol. 67, no. 11, pp. 4622 –4631, Nov. 2019.
- [26] H. Ren, H. Zhang, P. Li, Y. Gu, and B. Arigong, "A novel planar Nolen matrix phased array for MIMO applications," *IEEE International Symposium on Phased Array System & Technology (PAST)*, Waltham, MA, USA, pp. 1–4, 20. Oct 2019.
- [27] P. Li, H. Ren, and B. Arigong, "A symmetric beam -phased array fed by a Nolen matrix using 180° couplers," *IEEE Microw. Wireless Compon. Lett.*, vol. 30, no. 4, pp. 387 –390, Apr. 2020.
- [28] H. Ren, H. Zhang, and B. Arigong, "Ultra -compact 3 × 3 Nolen matrix beamforming network," *IET Microw. Antennas Propag.*, vol. 14, no. 3, pp. 143 –148, Jan. 2020.
- [29] M. Zhou, J. Shao, B. Arigong, H. Ren, R. Zhou, and H. Zhang, "A varactor based 90° directional coupler with tunable coupling ratios and reconfigurable responses," *IEEE Trans. Microw. Theory Techn.*, vol. 62, no. 3, pp. 416 –421, Mar. 2014.
- [30] H. Ren, M. Zhou, Y. Gu, and B. Arigong, "A tunable transmission line with controllable phase shifting and characteristic impedance," *IEEE Trans. Circuits Syst. II, Exp. Briefs*, vol. 67, no. 10, pp. 1720 –1724, Oct. 2019.